

## Use of Onion-Like Carbon to Reinforce Carbon Composites

A. Galiguzov<sup>1\*</sup>, A. Malakho<sup>1</sup>, S. Minchuk<sup>2</sup>, L. Oktiabrskaya<sup>2</sup>, V. Lepin<sup>2</sup>

<sup>1</sup>Lomonosov Moscow State University, 1/11, MSU, Leninskie Gory, Moscow, 119991, Russia

<sup>2</sup>AO «NPO «SPLAV», 33, Shcheglovskaya zaseka, Tula, 300004, Russia

### Article info

*Received:*  
3 February 2018

*Received in revised form:*  
14 April 2018

*Accepted:*  
19 June 2018

### Abstract

Onion-like carbon reinforced carbon-carbon composite was fabricated, and the influence of onion-like carbon (OLC) on the microstructure and mechanical and friction properties was investigated by porosity analysis, scanning electron microscopy, three-point bending test, nanoindentation test and ring-on-ring friction test. The results show that the sample containing OLC has a higher flexural strength (by 7.3%) and compressive strength (by 29.3%), hardness (by 2.1 times) and apparent density (by 1.1%) and smaller open porosity (7.9% vs 9.8%) and mesopore volume, which is confirmed by porosity analysis and is attributed to improved fiber/matrix interface performance. The presence of OLC results in higher hardness and elastic modulus of carbon matrix under nanoindentation testing, which leads to modification of friction mechanism and a decrease in the wear rate under friction (by 3.3 times). Besides, OLC particles form self-lubricating film and show a graphitic carbon solid lubricant properties.

## 1. Introduction

Carbon fiber-reinforced carbon matrix composites (C/C composites) are widely used for the production of aircraft and automobile brakes, structural components, anti-ablation protection [1–2] and articles of chemical-resistant valves and pipes [3]. Coal tar pitch, synthetic pitch and thermosetting resin are important as binders for C/C composite production [3]. To modify the binder properties the following main solid carbon additives are applied: carbon black [1, 4–6], nanosilicon carbide [7], coke [1, 8], fine graphite powder [1, 9–10], nano-graphene [11], and multi-walled carbon nanotube [12–13]. In general, additives act as a nucleation point in binder polymerization [5] and increase carbon yield and the strength while decreasing net carbonization shrinkage of carbon matrix [1]. Besides, presence of carbon filler particles leads to interaction between the filler and the binder pitch and stress-graphitization of matrix char [14], which influences matrix microstructure, and, as a result, alters mechanical properties of C/C composites based on different matrix microstructure [15–16].

The present work reports the results of C/C composites modification by OLC. The source of

OLC was nanodiamond powder (NDP), which was added under matrix precursor modification. It is known that NDP starts to transform into the OLC at 1400 K, and full NDP-OLC transformation finishes at 1800–1900 K [17]. Besides, heating at higher temperatures leads to the formation of hollow OLC [18]. NDP and OLC demonstrate good performance for modification of polymer composites [19–20], but there is no data concerning matrix precursor modification by NDP or OLC for C/C composites production.

## 2. Experimental

### 2.1. Materials

Chopped PAN(polyacrylonitrile)-based carbon fiber was used as reinforcement in C/C composites. The average length, filament diameter, tensile strength, tensile modulus and coupling agent content of the carbon fiber used were 30 mm, 6.4  $\mu\text{m}$ , 5.24 GPa, 375 GPa and 1.8% w/w, respectively. Commercially available coal tar pitches namely Bx95KS (CV = 63–65%) and HP180M (CV = 81–83%) with softening points of 118.3 and 164.2 °C (by Ring-and-Ball method, ASTM D36/D36M – 14e1) supplied by RÜTGERS Group

\*Corresponding author. E-mail: [agaliguzov@yandex.ru](mailto:agaliguzov@yandex.ru)

(Germany) were used as a binder and an impregnator, respectively. Ultradispersed nanodiamond charge (nanodiamond powder, NDP) produced by detonation synthesis with particle size of  $< 500$  nm (Fig. 1) and BET surface area of  $21.9 \text{ m}^2/\text{g}$  was used as a source of OLC (see section «Sample preparation»).

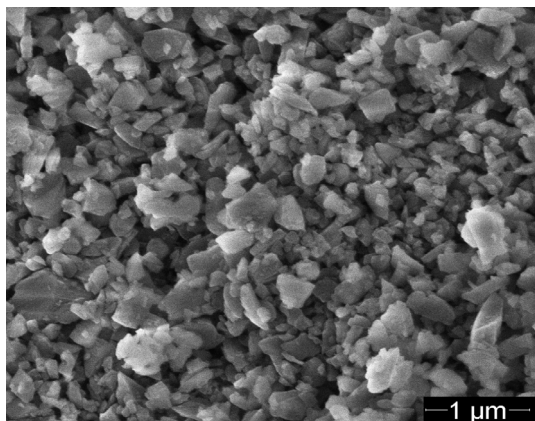


Fig. 1. SEM microphotograph of nanodiamond powder.

## 2.2. Sample preparation

To investigate the effect of ONC on C/C composite properties two types of samples were produced by preparation process shown in Fig. 2:

Type I (CC0): The binder was initial coal tar pitch (trademark – Bx95KS), while the impregnator was initial coal tar pitch (trademark – HP180M).

Type II (CC3): The binder was a modified pitch produced in the following way: ultradispersed nanodiamond charge was added to the initial binder pitch (Bx95KS) by intensive hot mixing using a Z-shaped blades mixer (Storverk, Russia) at the temperature of  $130\text{--}140$  °C and rotation rate of 30 rpm during 3 h under environmental conditions. The content of NDP was 3% w/w. The impregnator was initial coal tar pitch (trademark – HP180M). Softening point of the modified pitch did not change essentially after addition of nanodiamond and hot mixing and was  $118.7$  °C.

Carbon fiber content in both composite preforms was 25% w/w. It is important that the final temperature of composite samples heat treatment was  $2000$  °C, which leads to full transformation of NDP into OLC [18].

Two discs ( $550\text{--}30$  mm) produced following the preparation process shown in Fig. 2 were cut into samples of appropriate size/shape for corresponding tests.

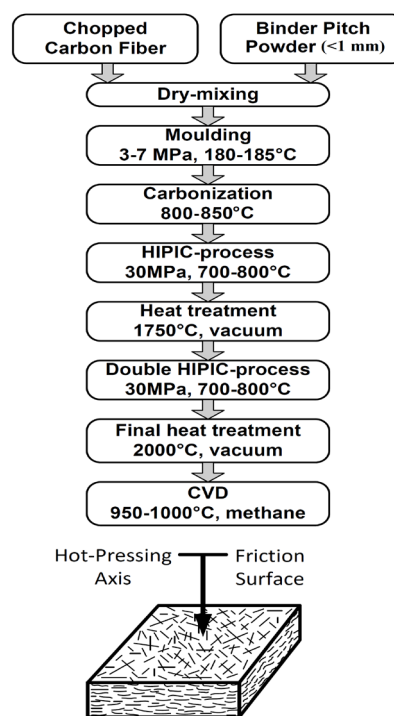


Fig. 2. General scheme of manufacturing process for C/C composites under study.

## 2.3. Binder and Composites Characteristics

### 2.3.1. Filler-Binder Interaction

To characterize chemical composition of initial and modified pitches (blend NDP and initial pitch) Fourier transform infrared (FTIR) spectroscopy was used. To estimate the interaction between the pitch and NDP thermogravimetric analysis and differential scanning calorimetry were applied. The former was performed with the help of a TG 209 F3 thermo-microbalance (Netzsch Group, Germany), which enables registering TG and DTG curves, while the latter was performed with a DSC 204 Phoenix (Netzsch Group, Germany).

### 2.3.2. C/C Composite Characteristics

To characterize the composites the following properties were determined:

a) Apparent density and open porosity of composites were defined by means of hydrostatic weighing according to ASTM C1039 – 85(2015).

b) Pore structure of composites was studied by low temperature nitrogen adsorption measurements. Adsorption measurements were made on a Thermo Electron Sorptomatic 1990 analyzer using grade A nitrogen (99.999% purity). Prior to measurements, the system was pumped down to a

residual pressure of  $\sim 10^{-1}$  Pa. In the course of measurements we used compact pieces cut from C/C composite material. The sample weight was approximately 5–7 g. Before adsorption process the material was outgassed at 423 K under vacuum of  $\sim 10^{-1}$  Pa.

c) Mechanical tests (flexural and compressive strength) were carried out on a universal testing machine (Hounsfield H5KS, UK). Rockwell hardness of samples friction surfaces were determined by microtribometer UMT-2 according to DIN 51917. Nanohardness test was performed by means of Nanoindentation Tester, NanoScan-3D (FSBI TISNCM, RF).

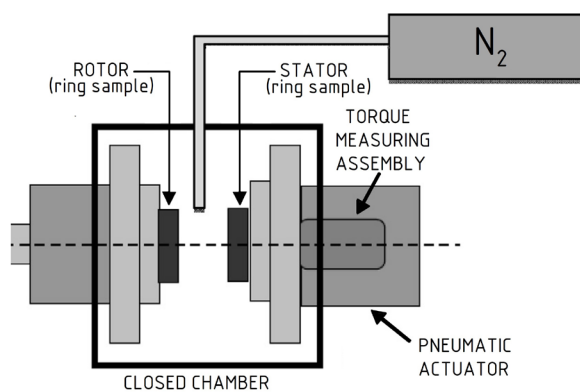


Fig. 3. Schematic diagram of subscale ring-on-ring.

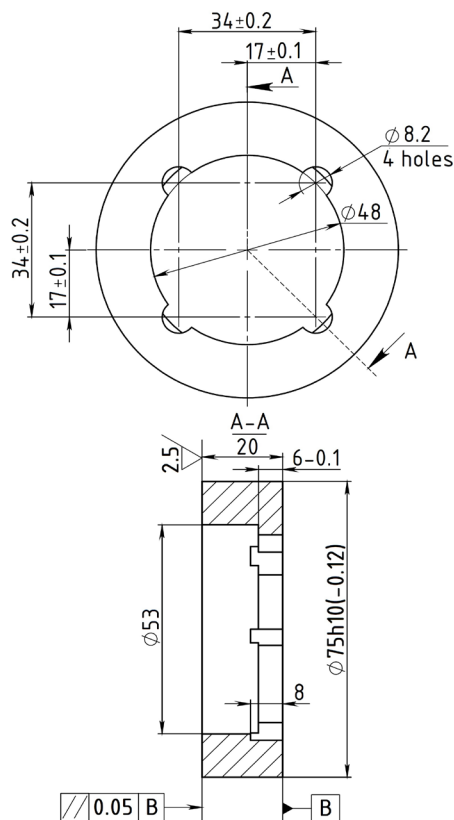


Fig. 4. Drawing of studied ring (stator and rotor).

d) Friction tests were performed in a normal air environment using an inertia type ring-on-ring configuration dynamometer (Fig. 3). The shape and size of studied rings (the stator as well as the rotor) are presented in Fig. 4. Friction coefficient and wear rate data were obtained.

e) The microstructure and friction surface morphology were studied by means of Quanta 3D FEG scanning electron microscopy (FEI, USA).

f) Microstructure analysis of cross-section surfaces of composites was carried out by means of Quanta 3D FEG scanning electron microscopy (FEI, USA) and composite surface images were processed by means of SemAfore 5.21 software.

### 3. Results and discussion

The results of mechanical, hardness and friction testing of C/C composites are illustrated in Table 1. Presence of OLC in C/C composite leads to an increase in average flexural and compressive strength and Rockwell hardness by 7.3%, 29.6% and 112.9%, respectively. It can be attributed to the decrease in open porosity by 19.4% [1] and change of pore structure.

As a rule, C/C composites show a rather high density and are not high porosity materials in terms of adsorption. According to scanning electron microscopy data (Fig. 5) C/C composites have a significant porosity. Their size ranges from hundreds of nanometers to several tens of microns. Such pores contribute very little to adsorption and hence are not taken into account by volumetric techniques.

Figure 6 shows the measured nitrogen adsorption/desorption isotherms for the C/C composites studied. According to low temperature nitrogen adsorption measurements adsorption/desorption isotherms of both types of composites are very similar. The shape of isotherms is typical of pore free and low porosity (from the viewpoint of adsorption) materials [21]. It indicates that there is no contribution to physisorption from a micro or mesoporous structure. At the same time, the adsorption hysteresis at high relative pressures ( $p/p^0 > 0.5$ ) suggests that the materials contain mesopores less than  $\sim 25$  nm in radius, which are involved in capillary condensation. The measured adsorption isotherms indicate that it can be attributed to type II in the BDDT classification [21] and allows evaluating specific surface area using BET analysis. The specific surface area of both types of C/C composites studied was the same and equaled  $\sim 0.69$  m<sup>2</sup>/g.

**Table 1**  
Characteristics of C/C composites produced

C/C type		CC0	CC3
NDP content, wt.%		0	3
Flexural strength, $\sigma_f$ , MPa		136.91 $\pm$ 5.70	146.85 $\pm$ 7.81
Compressive strength, $\sigma_c$ , MPa		163.71 $\pm$ 4.73	212.10 $\pm$ 5.82
Rockwell hardness		37.3 $\pm$ 2.3	79.4 $\pm$ 2.8
Apparent density, $\rho$ , g/cm <sup>3</sup>		1.81 $\pm$ 0.01	1.83 $\pm$ 0.01
Open porosity, P, vol.%		9.8 $\pm$ 0.7	7.9 $\pm$ 0.8
Friction performance	COF	0.305 $\pm$ 0.001	0.367 $\pm$ 0.026
	Wear rate, $\mu\text{m}/\text{stop}$	3.3 $\pm$ 0.4	1.0 $\pm$ 0.5
Nanoindentation testing			
Fiber	Hardness, H, GPa	2.0	2.7
	Elastic modulus, E, GPa	18	23
	Plastic index parameter, H/E	0.11	0.12
	Resistance to the plastic deformation, $H^3/E^2$ , GPa	0.025	0.037
Matrix	Hardness, H, GPa	0.5	1.7
	Elastic modulus, E, GPa	9.3	16.7
	Plastic index parameter, H/E	0.05	0.10
	Resistance to the plastic deformation, $H^3/E^2$ , GPa	0.001	0.018

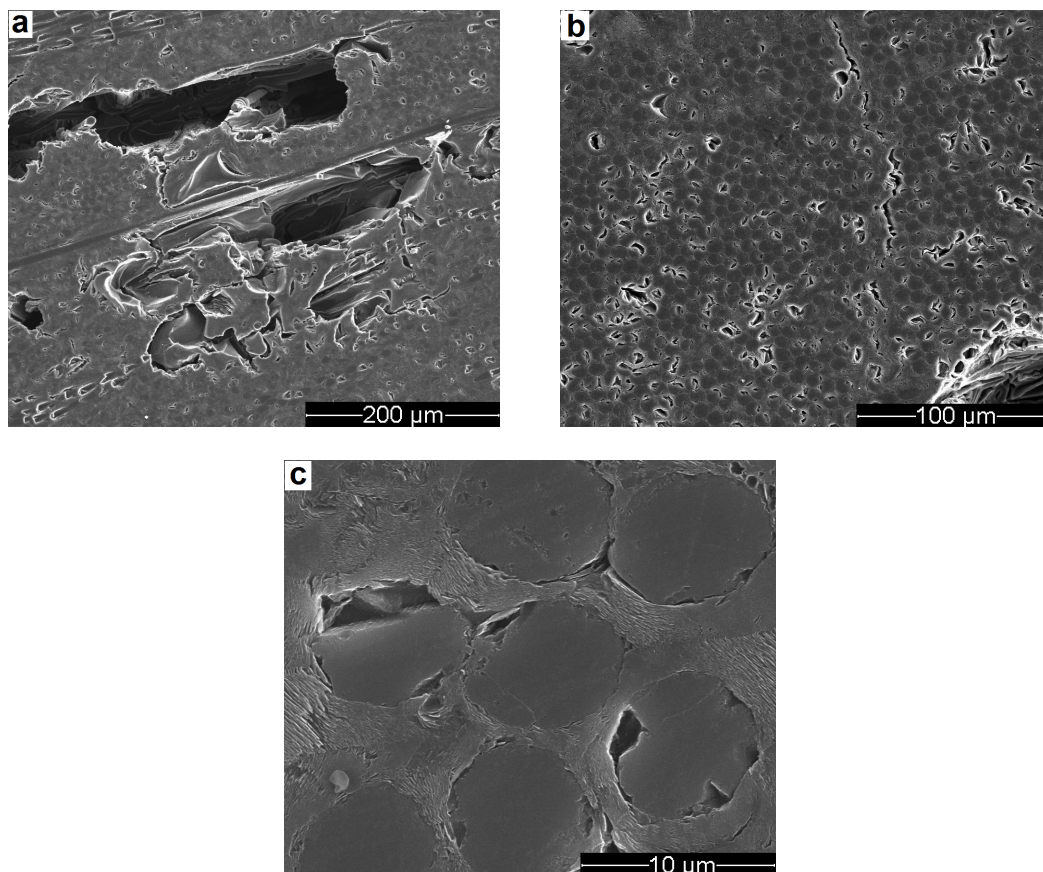


Fig. 5. Cross-sectional scanning electron microscope images of the C/C composites at different magnifications.

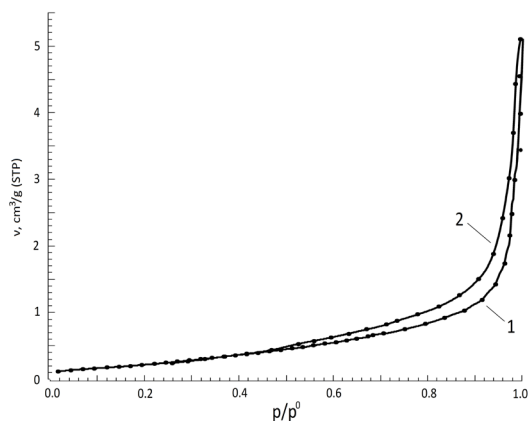


Fig. 6. 77 K nitrogen (1) adsorption and (2) desorption isotherms of C/C composites.

Small values of specific surface area confirm that there is no contribution to adsorption from a micro or mesoporous structure. The values of mesopore volume in the range of pore radii from 1 to 25 nm were evaluated by the Barrett-Joyner-Halenda method [22] using a desorption isotherm at relative pressures from 0.35 to 0.95 and were found to be  $\sim 0.0025$  and  $0.0019$   $\text{cm}^3/\text{g}$  for CC0 and CC3, respectively.

The pore structure of the C/C composite is formed largely by macropores. According to density/porosity analysis by hydrostatic method (ASTM C1039 – 85(2015)), open porosity for CC0 and CC3 composites is  $9.8 \pm 0.7$  and  $7.9 \pm 0.8$  (%), respectively, while the volume of open pores of CC0 and CC3 composites is  $0.0541$  and  $0.0428$   $\text{cm}^3/\text{g}$ .

The first stage of gaps and pores development is matrix carbonization. During baking the carbon preform (carbon fiber reinforced plastic) the melting and carbonization of matrix precursor take place and chemical bonding between fiber surface and functional groups of matrix precursor is rearranged. Fiber-matrix precursor bonding leads to carbon matrix shrinkage [23].

To investigate the influence of NDP on the matrix precursor and carbon matrix during melting and carbonization stages DSC and TGA analyses and FTIR spectroscopy were carried out. According to DSC analysis (Fig. 7), at low temperature interval ( $< 300$  °C) there are several endothermic peaks. Presence of NDP in the coal tar pitch does not change the melting point and the transition temperature from brittle to viscoelastic state: melting point/transition temperature for initial and modified coal tar pitches were  $64.0/113.6$  °C and  $64.8/112.8$  °C, respectively. But modified pitch showed additional endothermic peak at  $259.6$  °C, which can be explained by easier evaporation

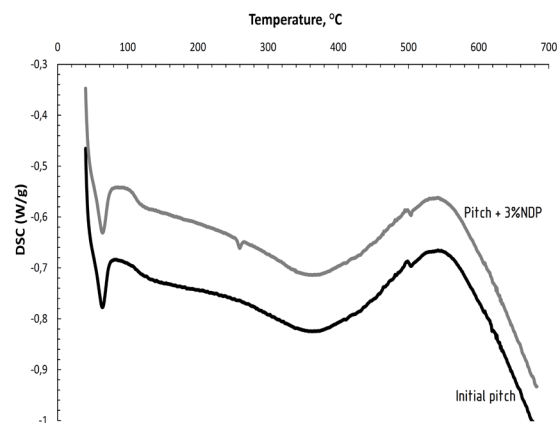


Fig. 7. DSC curves of initial pitch and pitch modified by NDP.

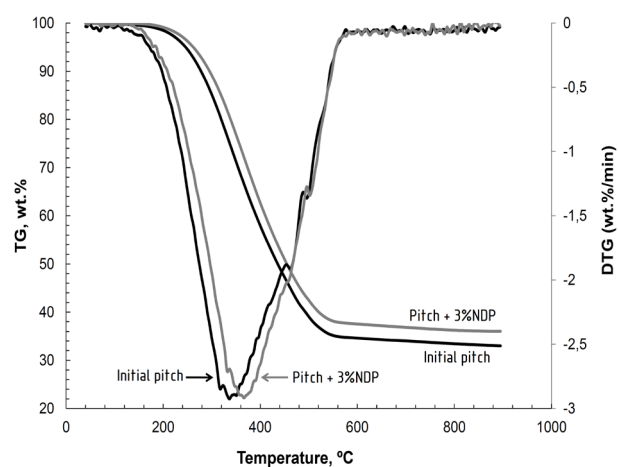


Fig. 8. TG and DTG curves of initial pitch and pitch modified by NDP.

of volatile pitch constituents, and NDP particles were evaporation nucleus. Above  $300$  °C several physico-chemical changes (polymerization, condensation, cracking, isomerization, molecular rearrangements, aromatization) are known to take place. These changes are characterized by wide exothermic peak at  $350$ – $650$  °C, and exothermic peak for modified pitch was very similar to the initial pitch.

According to TGA analysis (Fig. 8), presence of NDP leads to a slight increase in the weight loss onset temperature ( $197.8$  vs  $198.7$  °C for initial and modified pitch, respectively) and a mass change at the temperature of  $950$  °C ( $66.9$  vs  $63.9\%$  w/w, for initial and modified pitch, respectively), while temperature of maximum rate of mass loss does not change ( $367.5$  °C). The presence of NDP in coal tar pitch slightly increases carbon residue of modified coal tar pitch when compared to initial pitch, and the change agrees with the rule of mixtures for carbon residue provided that NDP is uncarbonizable.

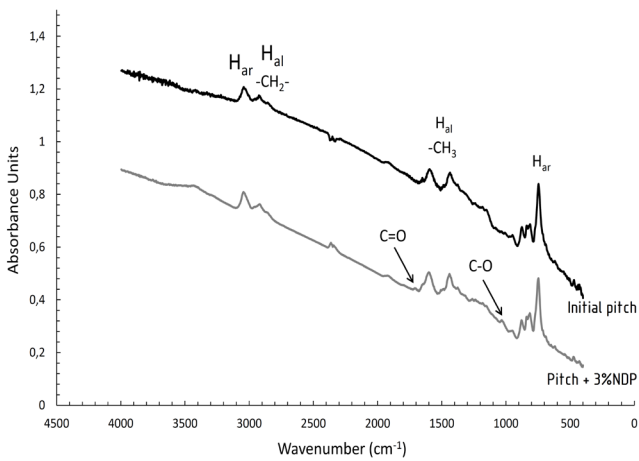


Fig. 9. FTIR spectra of initial pitch and pitch modified by NDP.

FTIR spectroscopy revealed that the spectra of initial and modified coal tar pitches were very similar (Fig. 9), the only difference being that the spectrum of modified pitch showed weak bands associated with presence of a C=O group ( $1725\text{--}1700\text{ cm}^{-1}$ ) and C-O group ( $1075\text{--}1025\text{ cm}^{-1}$ ), which can be explained by partial oxidation of coal tar pitch under modification with NDP [7]. Overall, no evidence of any type of chemical interaction between the NDP and coal tar pitch has been found.

Presence of OLC lead to a threefold decrease in linear wear rate under friction testing, which is likely to be connected with: 1) matrix mechanical performance; 2) matrix frictional profile; 3) change of friction surface morphology.

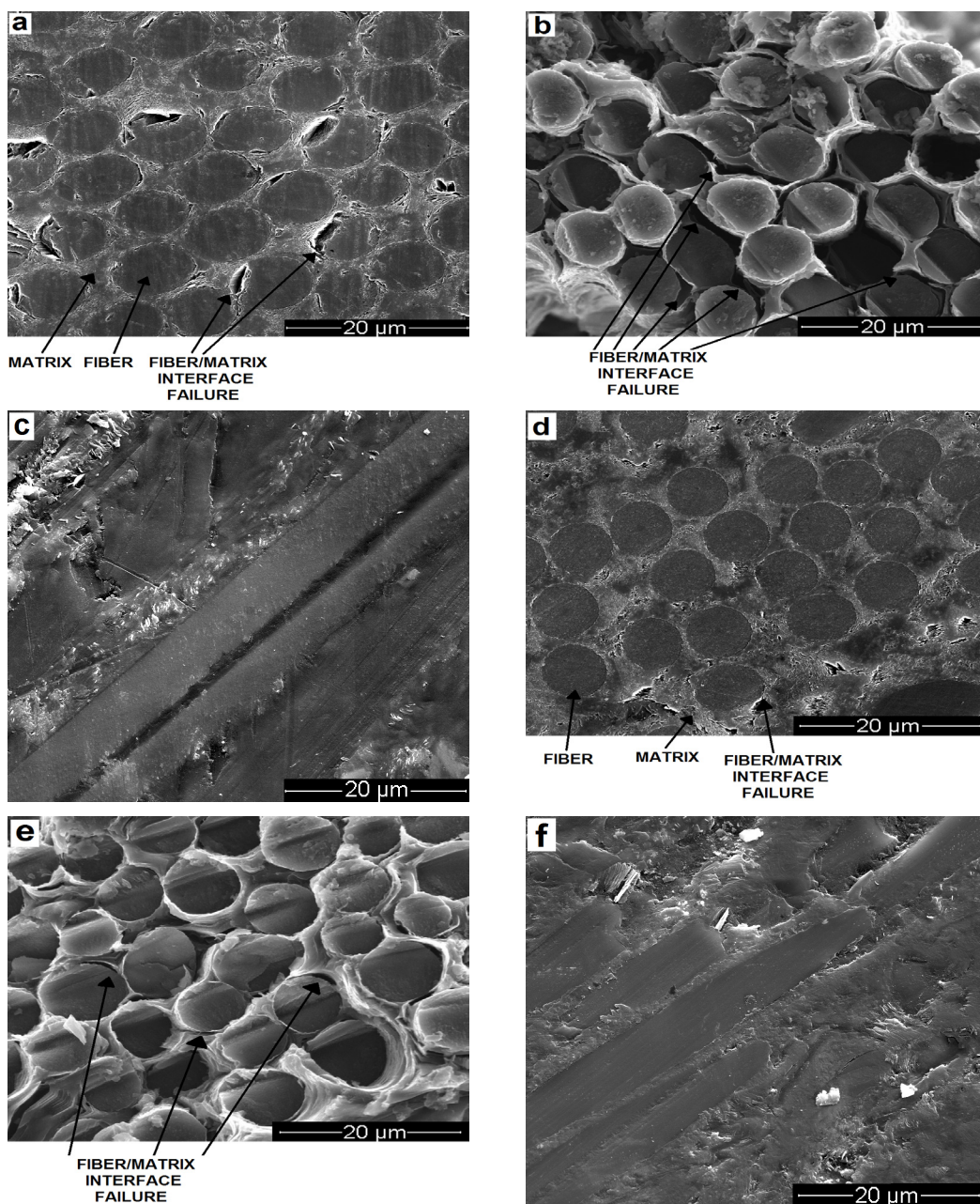


Fig. 10. SEM observation of cross-section surface, fracture face after flexural strength testing and friction surface: (a), (b), (c) – for CC0 composite and (d), (e), (f) – for CC3 composite, respectively.

1) As shown in Table 1, hardness and elastic modulus of matrix for CC3 composite increased by 3.4 and 1.8 times, respectively, in comparison with CC0 composite, which lead to the growth of plastic index parameter and resistance to the plastic deformation (RPD) in 2 and 18 times, respectively. It can be connected both with additional matrix reinforcement by NDP/OLC and decrease in the number and size of gaps between fiber and matrix and cracks which developed under carbonization shrinkage, which significantly increases mechanical properties of matrix and composite [9].

According to microstructural analysis of cross-section surfaces (Fig. 10 (a) and (d)) and fracture surfaces (Fig. 10 (b) and (e)), the composites showed presence of annular gaps between the fiber and the matrix, but the size, the number of gaps and their surface area are larger for CC0 composite: the surface area value of the gaps was estimated using SemAfore 5.21 software as shown in Fig. 11 in accordance with equation and was on average 8.6% higher in comparison with CC3 composite (8.1% for CC0 vs 8.8% for CC3). Overall sample surface was 4 square centimeters for each composite.

$$P_G = \frac{S_G}{S_0} \times 100\%$$

where  $P_G$  – surface area percent of gaps between fiber and matrix,  $S_G$  – surface area of gaps between fiber and matrix on the image under consideration,  $S_0$  – whole surface area of image under consideration.

2) The decrease in linear wear rate for CC3 composite can be caused by modification of friction mechanism in presence of OLC particles. OLC is known to produce low friction coefficients and wear rates both in air and in vacuum [24], and it is a graphitic carbon solid lubricant which

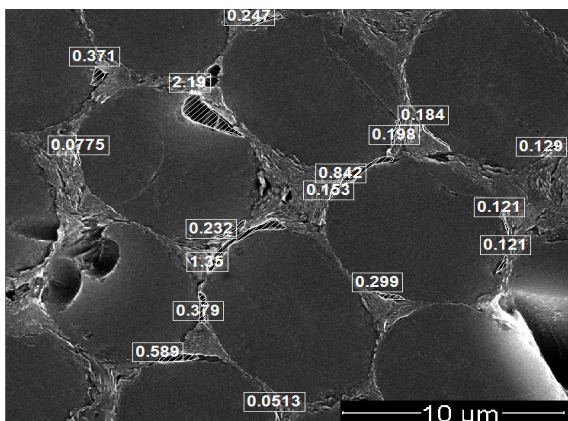


Fig. 11. Scheme of determination of surface area of the gap between fiber and matrix (values are given in square  $\mu\text{m}$ ).

forms a self-lubricating friction film under C/C composite tribological testing [25]. Formation of graphitic carbon solid lubricant film (in case of CC3 composite) is also connected with presence of higher content of graphite-like matrix as compared with CC0 composite. It results from stress graphitization of matrix under high temperature treatment. It often occurs at the interfaces between different phases, particularly the binder and the filler [14].

3) According to Fig. 10 (c) and (f), Fig. 12 (a)-(b), samples showed different surface asperity; their surface contains fibers and matrix components. Surface asperity for CC0 and CC3 is 0.7 and 0.12  $\mu\text{m}$ , respectively, which is related to friction mechanism modification. Under composite friction testing the difference between fiber RPD and matrix RPD is important. For CC0 composite RPD of fiber is 25 times higher compared to RPD of matrix, while for CC3 composite RPD of fiber is only 2 times higher than RPD of matrix. It results in a state when harder PAN fiber particles cause a significant wear of a softer carbon matrix during friction process [26].

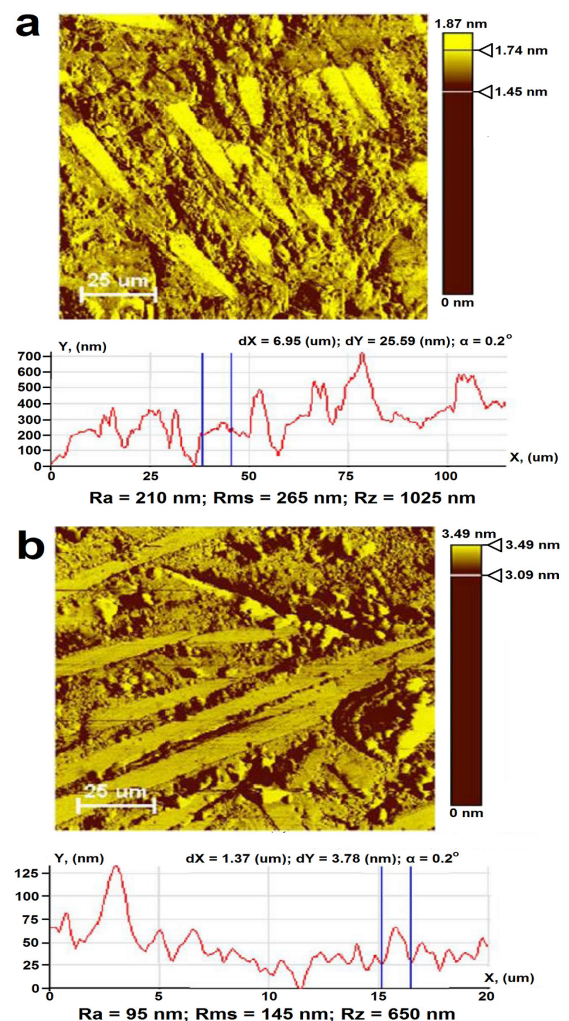


Fig. 12. Friction surface contour plot of CC0 (a) and CC3 (b) composites.

#### 4. Conclusions

Onion-like carbon reinforced C/C composite was fabricated. The source of OLC was nanodiamond powder (NDP), 3% w/w of which was added to the binder pitch under green preform preparation. Final heat treatment temperature of C/C composite was 2000 °C. The results showed that the presence of OLC influenced several characteristics of C/C composite. OLC reinforced C/C composite exhibited lower open porosity in comparison with non-modified composite (7.9 vs 9.8, respectively) and a smaller volume of open pores than the one without OLC by 24.0% and 26.4%, respectively, with BET specific surface area being the same for both types of C/C composites. The decrease of OLC reinforced composite porosity was connected with a decrease in the number and size of gaps between fiber and matrix and cracks which developed under carbonization shrinkage. As a result, OLC reinforced composite showed improved mechanical profile. Presence of OLC enhanced friction performance, in particular, the modified composite demonstrated smaller wear rate under ring-on-ring friction testing as compared to non-modified composite (1.1 vs 3.3, respectively), which was connected with friction mechanism modification by OLC particles which acted as a graphitic carbon solid lubricant.

#### Acknowledgements

The research was supported by the Ministry of Education and Science of the Russian Federation, Resolution № 218, 9 April, 2010 (contract No. 02.G25.31.0169 «Development of Technology for Heat-Resistant and Chemically Resistant Composites for Pipeline Parts» of JSC Splav and Lomonosov Moscow State University).

#### References

[1]. E. Fitzer, L.M. Manocha, Applications of Carbon/Carbon Composites. In: Carbon Reinforcements and Carbon/Carbon Composites. Springer, Berlin, Heidelberg; 1998. DOI: 10.1007/978-3-642-58745-0\_10

[2]. S. Awasthi, J.L. Wood, *Ceram. Eng. Sci. Proc.* 9 (7-8) (1988) 553–560. DOI: 10.1002/9780470310496.ch4

[3]. P. Morgan, Carbon Fibers and Their Composites. Boca Raton, FL: Taylor & Francis; 2005. DOI: 10.1201/9781420028744.ch14

[4]. D.D.L. Chung, Carbon Fiber Composites. Elsevier Inc. 1994. DOI: 10.1016/C2009-0-26078-8

[5]. R. Menendez, J.J. Fernandez, J. Bermejo, V. Cebolla, I. Mochida, Y. Korai, *Carbon*

34 (7) (1996) 895–902. DOI: 10.1016/0008-6223(96)00044-9

[6]. G. Bhatia, R.K. Aggarwal, *J. Mater. Sci.* 16 (7) (1981) 1757–1762. DOI: 10.1007/BF00540621

[7]. D. Mikociak, A. Magiera, G. Labojko, S. Blazewicz. *J. Anal. Appl. Pyrol.* 107 (2014) 191–196. DOI: 10.1016/j.jaap.2014.03.001

[8]. R.K. Aggarwal, G. Bhatia, O.P. Bahl, *J. Mater. Sci.* 22 (5) (1987) 1630–1634. DOI: 10.1007/BF01132384

[9]. E. Yasuda, Y. Tanabe, *Carbon* 26 (2) (1988) 225–227. DOI: 10.1016/0008-6223(88)90041-3

[10]. T.J. Kang, Y.W. Jeong, *Polym. Polym. Compos.* 5 (1997) 469–475.

[11]. D. Bansal, S. Pillay, U. Vaidya, *Carbon* 55 (2013) 233–244. DOI: 10.1016/j.carbon.2012.12.032

[12]. X. Gao, L. Liu, Q. Guo, J. Shi, G. Zhai, *Mater. Lett.* 59 (2005) 3062–3065. DOI: 10.1016/j.matlet.2005.05.021

[13]. D.S. Lim, J.W. An, H.J. Lee, *Wear* 252 (2002) 512–517. DOI: 10.1016/S0043-1648(02)00012-1

[14]. M. Inagaki, F. Kang, M. Toyoda, H. Konno, *Advanced Materials Science and Engineering of Carbon*. Oxford: Elsevier Inc.; 2014; p. 109.

[15]. F. Dillon, K.M. Thomas, H. Marsh, *Carbon* 31 (8) (1993) 1337–1348. DOI: 10.1016/0008-6223(93)90095-R

[16]. R. Menendez, E. Casal, M. Granda, Chapter 7, *Fibers and Composites* (Ed. P. Delhaes), London: Taylor & Francis; 2003.

[17]. Z. Qiao, J. Li, N. Zhao, C. Shi, P. Nash, *Scripta Mater.* 54 (2006) 225–229. DOI: 10.1016/j.scriptamat.2005.09.037

[18]. V. Kuznetsov, Y. Butenko, *Synthesis, Properties and Applications of Ultrananocrystalline Diamond* 192 (2005) 199–216. DOI: 10.1007/1-4020-3322-2\_15

[19]. O. Shenderova, C. Jones, V. Borjanovic, S. Hens, G. Cunningham, S. Moseenkov, V. Kuznetsov, G. McGuire, *Phys. Stat. Sol. (a)* 205 (9) (2008) 2245–2251. DOI: 10.1002/pssa.200879706

[20]. S.A. Rakha, R. Raza, A. Munir, *Polym. Composite* 34 (6) (2013) 811–818. DOI: 10.1002/pc.22480

[21]. S.J. Gregg, K.S.W. Sing, *Adsorption, Surface Area and Porosity*. New York: Academic; 1982.

[22]. E.P. Barrett, L.G. Joyner, P.P. Halenda, *J. Am. Chem. Soc.* 73 (1951) 373–380. DOI: 10.1021/ja01145a126

[23]. G. Savage, *Carbon-Carbon Composites*. Springer Netherlands; 1993. DOI: 10.1007/978-94-011-1586-5

[24]. A. Hirata, M. Igarashi, T. Kaito, *Tribol. Int.* 37 (11-12) (2004) 899–905. DOI: 10.1016/j.triboint.2004.07.006

[25]. H. Marsh, E.A. Heintz, F. Rodriguez-Reinoso, *Introduction to carbon technologies*. Alicante: University of Alicante; 1997; p. 624.

[26]. S. Ozcan, P. Filip, *Carbon* 62 (2013) 240–247. DOI: 10.1016/j.carbon.2013.05.061